ISSN: 0975-833X

Available online at http://www.journalcra.com

International Journal of Current Research
Vol. 18, Issue, 07, pp.37932-37942, July, 2026
DOI: https://doi.org/10.24941/ijcr.50750.07.2026

INTERNATIONAL JOURNAL OF CURRENT RESEARCH

RESEARCH ARTICLE

PARAMETRIC STUDY OF A FLAT-PLATE AIR SOLAR COLLECTOR USING RECYCLED DRINKS CANS AS AN ABSORBER

Salifou Tera[1], Souleymane Sinon[2], Kalil Pierre Mathos[1], Maurice Faya Yombouno[1], Mamadi Diakite[1], Madani Thierno Sidibé[3] and Oumar Sanogo[2]

[1]Département de Physique, Faculté des Sciences et Techniques, Université de Nzérékoré, NZérékoré, République de Guinée; [2]Institut de Recherche en Sciences Appliquées et Technologies, Centre National de la Recherche Scientifique et Technologique (IRSAT/CNRST), Ouagadougou, Burkina Faso; [3]Laboratoire des Energies Hybrides et Renouvelables (HREL), Faculté des Sciences et Techniques (FST), Université des Sciences, Techniques etTechnologies de Bamako (USTTB), Mali

ARTICLE INFO

Article History:
Received 17th April, 2026
Received in revised form
20th May, 2026
Accepted 27th June, 2026
Published online 30th July, 2026

Keywords:

Solar Energy, Solar Collector, Modelling, Heat transfer.

**Corresponding author: Salifou Tera*

ABSTRACT

In this article, a numerical study of a solar collector made from aluminum cans is carried out to determine the optimal performance and design parameters of this system for converting solar radiation into thermal energy. The collector is coupled with a drying chamber for drying fruit and vegetables. It consists of three main components, namely a transparent cover (glass), and an absorber that also serves as a conduit for the heat transfer fluid (made from aluminum beverage cans). Transient modelling is used to characterize the dynamic behaviour of the collector. The model developed was established on the basis of energy conservation equations using the nodal method. A set of equations representing the model is solved simultaneously using SCILAB simulation software. The results are validated withexperimental data and then used to investigate the influence of various parameters on the collector's performance, such as the mass flow rate of air at the collector inlet, the length of the columns of can tubes, and the number of holes at the outlet of each can. The results showed that the fluid temperature at the solar collector outlet decreases as the air flow rate at the solar collector inlet increases, whilst the daily thermal yield increases with the increase in air flow rate.The results also indicate that the solar collector performs best with can tubes featuring two (02) 1-centimetre-diameter holes in terms of both outlet fluid temperature and efficiency.

Citation: **Salifou Tera, Souleymane Sinon, Kalil Pierre Mathos, Maurice Faya Yombouno, Mamadi Diakite, Madani Thierno Sidibé, Oumar Sanogo, *2026.*** "Parametric study of a flat-plate air solar collector using recycled drinks cans as an absorber". ***International Journal of Current Research, 18, (07), 37932-37942.***

INTRODUCTION

Solar energy in all its forms plays a vital role in economic and industrial development. Owing to its economic and environmental benefits, solar energy converted into heat has found numerous applications in the fields of space heating, drying, cooling, etc. ((1), (2)). Flat-plate air collectors are among the devices that convert solar energy into heat drawn from the flow of air through the solar collector. Solar thermal collectors are designed to convert the sun's radiant energy directly into thermal energy, based on the greenhouse effect. They consist mainly of a transparent cover (made of glass or plastic) that captures solar radiation, an absorber usually painted black to absorb as much solar radiation as possible an air duct, and thermal insulation. The design of a solar collector offers advantages in terms of its simple structure, low manufacturing cost and low maintenance requirements. However, the thermal efficiency of these air-based solar collectors remains very low due to the thermophysical properties of air, which are significantly lower than those of liquid heat transfer fluids. These physical properties affect the convective heat transfer coefficient between the air and the absorber (3). One of the methods used to increase the convective heat transfer rate between the air flow and the absorber involves modifying the geometry of the heat transfer fluid flow ((4), (5)). The methods employed have mainly involved the application of artificial roughness elements or corrugated plates within the air duct, the installation of internal fins attached to the absorber plate, and the external and internal recirculation of air to enhance the thermal performance of these systems (3). Several designs featuring different shapes and dimensions for the heat transfer fluid flow path within flat-plate solar collectors have been developed and tested (6). A. Abene et al. (7) investigated a flat-plate solar collector fitted with several types of obstacles arranged in rows within the dynamic air flow. The study compared a flat-plate solar collector with obstacles to one without obstacles. The results show a marked improvement in heat transfer, the outlet temperature of the heat transfer fluid and the thermal efficiency of the air-side flat-plate solar collector with the different types of obstacles.H.M. Yeh et al(8) conducted experimental and analytical studies on the efficiency of a finned dual-flow air-side solar collector. The results show an increase in the thermal efficiency of the finned air-side solar collector. Ozgen et al(9) conducted an experimental study on the thermal performance of a dual-flow solar collector equipped with aluminum beverage cans as an absorber. Three different absorber plates were tested as part of their study.In the first type (Type I), the cans were arranged in a zigzag pattern on the absorbent plate, whereas in Type II, they were arranged in an orderly fashion. Type III consists of a flat plate (without cans). Experiments were carried out at air mass flow rates of 0.03 kg/s and 0.05 kg/s. The results showed that the highest efficiency was achieved for type I at 0.05 kg/s.Sinon et al. (10) conducted an experimental study of heat transfer via forced convection in a flat-plate air-side solar collector with an absorber made from aluminum drinks cans. The results showed an increase in the turbulence of the heat transfer fluid and an improvement in the thermal efficiency of the solar collector designed for use in the food industry. The aim of this study is to use a numerical model to determine the influence of certain design parameters in order to optimize the thermal performance of the air-type solar collector. Parameters such as the length of the tube columns, the air flow rate at the solar collector inlet and the number of holes will be studied in relation to the air temperature at the outlet and the daily thermal efficiency of the solar collector, with a view to providing an optimal design for such a flat-plate solar collector.

Description of the experimental setup: The solar collector under consideration in this study is a glazed flat-plate air-side solar collector (Figure 1) operating on the principle of forced convection. It consists mainly of a frame, an absorber and a glass pane (3 mm thick). The frame of our collector is made of two aluminum sheets measuring 2600 mm × 600 mm × 50 mm, between which lies a 5 cm thick layer of glass wool, serving as insulation for the collector.The absorber is made from aluminum drinks cans painted black to increase their ability to absorb solar radiation. Each can has a 5 cm diameter hole drilled into its top through which cool air enters, and three (03) holes, each 1 cm in diameter, drilled into its bottom through which hot air exits (Figure 2). The holes are arranged on the two opposite sides so as to generate turbulence within the cans. This improves convective heat transfer between the heat transfer fluid and the inner walls of the cans. The cans were then assembled into columns (nine in total), thus forming absorber tubes.A total of 153 cans were used to construct the solar collector. The collector was mounted on a support inclined at an angle of 12° to the horizontal and oriented towards the south in accordance with the site's latitude. The dimensions and specifications of the solar collector are shown in Table 1 below.

Figure 1. Scheme of the solar collector

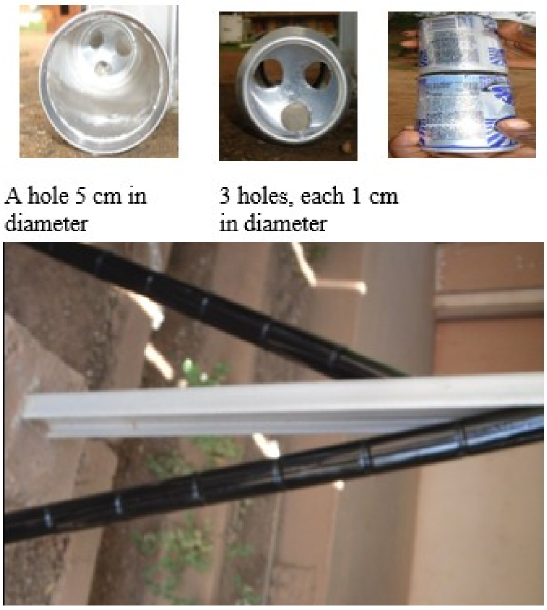

Figure 2. Description of the can tubes

Table 1: Solar collector specifications

Dimensions of the solar collector	2600x600x50(mm)
Thickness of the glass	3mm
Glass transmittance (τ_g)	0.9
Glass emissivity	0.85
Absorber tube diameter	50mm
Length of the absorber tubes	2600mm
Number of tube columns	9
Number of cans	153
Absorptivity of a matte black absorber (α_n)	0.95
Emissivity of the absorber	0.85
Thickness of the glass wool insulation	50mm
Thermal conductivity of insulating glass wool	0.042W/m.K

Modelling of a solar thermal collector

Physical model of the solar collector: Figure 3 illustrates the various physical phenomena that describe the thermal behaviour of the solar collector. The energy conservation equations for the air solar collector are described in terms of parameters such as the length of the tube columns, the air flow rate at the collector inlet and the number of holes, as well as the air temperature at the outlet and the thermal efficiency. To facilitate the solution of these equations, the following simplifying assumptions are made:

- The solar collector operates under transient conditions;
- The fluid flow is assumed to be unidirectional;
- Conduction within the absorber is assumed to be negligible as its thickness is considered sufficiently small (1 mm);
- Lateral heat losses from the solar collector are neglected;
- The air flow rate is assumed to be uniform at the inlet of each column of can tubes;
- The physical properties of the materials are independent of temperature.

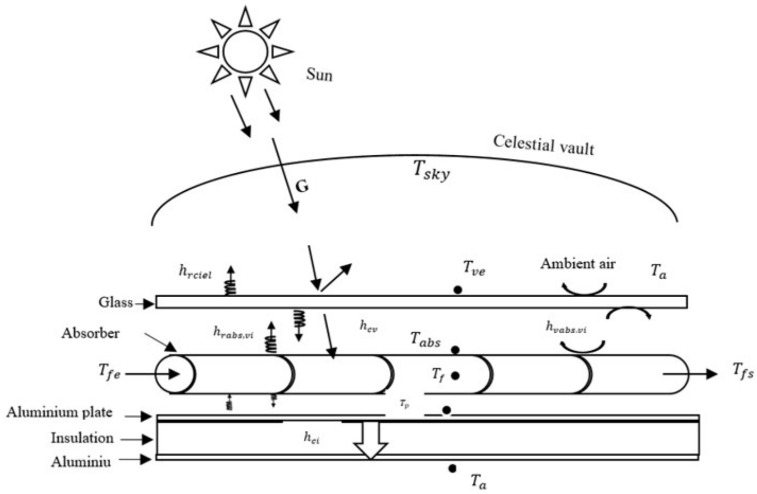

Figure 3. Different types of heat transfer within the air-side solar collector

3.2 Energy conservation equations for solar collectors

To establish the mathematical model of our solar collector, the thermal energy balance method is applied to each component of the collector. These balances reflect the conservation of thermal energy for each component by applying the nodal method, in which each component is treated as a node to which temperatures are applied:

- At the glass pane

The heat balance of the glass pane is defined by equation (1), which can be rewritten as follows:

$$\rho_g V_g C_{Pg} \frac{dT_g}{dt} = \alpha_g G S_g + h_{amb} S_g \left(T_a - T_g\right) + h_{r,sky} S_g \left(T_{sky} - T_g\right) + S_n \left(h_{v,n-g} + h_{r,n-g}\right)\left(T_n - T_g\right)$$

(1)

- At the absorber (aluminum can)

The heat balance of the drink can absorber is defined by equation (2) as follows:

$$\rho_n V_n C_{pn} \frac{dT_n}{dt} = \alpha_n \tau_g G S_n + S_n \left(h_{r,n-g} + h_{v,n-g}\right)\left(T_g - T_n\right) + h_{r,n-g} S_n \left(T_p - T_n\right) + h_{v,n-f} S_{n-f} \left(T_f - T_n\right)$$

(2)

- With regard to the heat transfer fluid

The heat balance for a can tube column element is defined by equation (3):

$$\rho_f V_f C_{pf} \left(\frac{dT_f}{dt} + u_f \frac{dT_f}{dx}\right) = h_{v,n-f}\left(T_n - T_f\right)$$

(3)

- At the plate level

The heat balance of the aluminum sheet beneath the absorber is defined by equation (4) as follows:

$$\rho_p V_p C_{p_p} \frac{dT_p}{dt} = h_{r,n-p} S_n \left(T_n - T_p\right) + h_{ci} S_p \left(T_{amb} - T_p\right) \tag{4}$$

Determination of the overall heat loss coefficient: The calculation of heat loss coefficients is fundamental to assessing the performance of a flat-plate solar collector. The overall heat loss coefficient (U_L) of the collector is the sum of the front(U_{av}) and rear (U_{ar}) heat loss coefficients (Equation 5), with lateral losses assumed to be negligible. This heat loss occurs between the solar collector and its surroundings via conduction, convection and infrared solar radiation.

$$U_L = U_{av} + U_{ar} \tag{5}$$

The overall heat loss coefficient towards the front of the solar collector is given by equation (6):

$$U_{av} = \frac{1}{\frac{1}{h_{amb}+h_{r,sky}} + \frac{e_g}{\lambda_g}} \tag{6}$$

The overall heat loss coefficient towards the rear of the solar collector is very small compared to that of heat losses towards the front, as the solar collector is very well insulated at the rear. It is expressed as follows (Equation (7)):

$$U_{ar} = \frac{\lambda_{iso}}{e_{iso}} \tag{7}$$

Determination of heat transfer coefficients

Convective heat transfer coefficients

• The convective heat transfer coefficient between the glass and the ambient air is given by the correlation proposed by McAdams 1954 [11].

$$h_{amb} = 5{,}67 + 3{,}86 u_{amb} \tag{8}$$

Where u_{amb} is the wind speed

$$h_{v,n-g} = \frac{Nu\lambda_f}{e_{ac}} \tag{9}$$

Where e_{ac} is the thickness of the blade layer between the absorber and the glass, and λ_f is the thermal conductivity of air. The dimensionless Nusselt number (Nu) is given by the following correlation [12]:

$$Nu = 1 + 1.44\left[1 - \frac{1708}{Ra.cosi}\right]^* \left[1 - \frac{1708(sin1.8i)^{1.6}}{Ra.cosi}\right] + \left[\left(\frac{Ra.cosi}{5830}\right)^{1/3} - 1\right]^* \tag{10}$$

This Nusselt correlation applies to values between 0° and 60°C, which represents the angle of inclination of the solar collector relative to the horizontal plane. The dimensionless Rayleigh number Ra is expressed by equation (11).

$$Ra = \frac{g\beta\Delta T e_{ac}^3}{\nu\kappa} \tag{11}$$

With β the coefficient of thermal expansion in K^{-1},ΔT the temperature difference between the glass and the absorber in K , g the gravitational field in m^2/s , ν the kinematic viscosity in m^2/s , and κ the thermal diffusivity m^2/s .

• The convective heat transfer coefficient between the heat transfer fluid and the absorber walls is given by equation (12):

$$\boldsymbol{h_{v,n-f} = \frac{Nu\lambda_f}{D_c}} \tag{12}$$

The Nusselt number for transient flow is given by the correlation proposed [11]:

$$Nu = 0.027Re^{0.8}Pr^{0.33} \tag{13}$$

The expressions for the dimensionless numbers the Reynolds number and the Prandtl number are given in equations (14) and (15) respectively.

$$Re = \frac{\rho_f u_f D_c}{\mu_f} \tag{14}$$

$$Pr = \frac{\mu_f c_{p_f}}{\lambda_f} \tag{15}$$

Where Re and Pr are the dimensionless Reynolds and Prandtl numbers respectively,ρ_f the density of the fluid (air) in kg/m^3, D_c the hydraulic diameter of the can tubes in m, μ_f the dynamic viscosity in $kg/(m.s)$; $C_{p_f}$the specific heat capacity of the fluid in J/kg and λ_f the thermal conductivity of the fluid in $W/(m.K)$.

The radiative transfer coefficients

• The radiative transfer coefficient between the glass and the sky is calculated using the following formula:

$$h_{r,sky} = \frac{\sigma\left(T_{sky}+T_g\right)\left(T_{sky}^2+T_g^2\right)}{\left(\frac{1}{\varepsilon_g}\right)} \tag{16}$$

Where $\sigma = 5.67 \times 10^{-8} W/m^2K^4$ is the Stefan-Boltzmann constant and ε_g is the emissivity of the glass. The sky temperature T_{sky} is given by the following correlation [13]:

$$T_{sky} = 0.0552\left(T_{amb}\right)^{1.5} \tag{17}$$

• The heat flux exchanged by radiation between the glass pane and the absorber can be expressed using the equation below.

$$h_{r,sky} = \frac{\sigma\left(T_{sky}+T_g\right)\left(T_{sky}^2+T_g^2\right)}{\left(\frac{1}{\varepsilon_g}\right)} \tag{18}$$

Together with the absorber's emissivity.

Method of resolution: The time terms in the solar collector's energy balance equations are discretized using the implicit Euler finite difference method (Equation (19)). The advection term in the fluid equation is discretized by taking the difference between two temperatures (Equation (20)).

$$\frac{\partial T}{\partial t} = \frac{T_i^{n+1} - T_i^n}{\Delta t} \tag{19}$$

$$\frac{\partial T}{\partial x} = \frac{T_i^{n+1} - T_{i-1}^{n+1}}{\Delta x} \tag{20}$$

The above equations can be written in the form of a 4×4 matrix equation, with matrix $[A]$, variable $[T]$ and right-hand side $[A]$, such that $[A] \times [T] = [B]$.

$$\begin{bmatrix} A_{11} & A_{12} & 0 & 0 \\ A_{21} & A_{22} & A_{23} & A_{24} \\ 0 & A_{32} & A_{33} & 0 \\ 0 & A_{42} & 0 & A_{44} \end{bmatrix} \begin{pmatrix} T_g^{n+1} \\ T_n^{n+1} \\ T_f^{n+1} \\ T_p^{n+1} \end{pmatrix} = \begin{pmatrix} B_1 \\ B_2 \\ B_3 \\ B_4 \end{pmatrix} \tag{21}$$

Where :

$$A_{11} = \frac{\rho_g V_g C_{pg}}{\Delta t} + S_g\left(h_{amb} + h_{r,sky}\right) + S_n\left(h_{r,g-n} + h_{v,g-n}\right) \tag{22}$$

$$A_{12} = A_{21} = -S_n\left(h_{r,g-n} + h_{v,g-n}\right) \tag{23}$$

$$A_{22} = \frac{\rho_n V_n C_{pn}}{\Delta t} + S_n\left(h_{r,g-n} + h_{v,g-n} + h_{r,n-p}\right) + h_{v,n-f} S_{n-f} \tag{24}$$

$$A_{11} = \frac{\rho_g V_g C_{pg}}{\Delta t} + S_g\left(h_{amb} + h_{r,sky}\right) + S_n\left(h_{r,g-n} + h_{v,g-n}\right) \tag{22}$$

$$A_{12} = A_{21} = -S_n\left(h_{r,g-n} + h_{v,g-n}\right) \tag{23}$$

$$A_{22} = \frac{\rho_n V_n C_{pn}}{\Delta t} + S_n\left(h_{r,g-n} + h_{v,g-n} + h_{r,n-p}\right) + h_{v,n-f} S_{n-f} \tag{24}$$

$$A_{23} = A_{32} = -h_{v,n-f} S_{n-f} \tag{25}$$

$$A_{24} = A_{42} = -h_{r,n-p} S_{n-p} \tag{26}$$

$$A_{33} = \frac{\rho_f V_f C_{pf}}{\Delta t} + \frac{\rho_f V_f C_{pf} u_f}{\Delta x} + h_{v,n-f} S_{n-f} \tag{27}$$

$$A_{44} = \frac{\rho_p V_p C_{p_p}}{\Delta t} + h_{r,n-p} S_n + h_{ci} S_p \tag{28}$$

$$B_1 = \alpha_g \mathrm{G} S_g + \frac{\rho_g V_g C_{pg}}{\Delta t} T_g^n + h_a S_g T_{amb} + h_{r,sky} S_g T_{sky} \tag{29}$$

$$B_2 = \alpha_n \tau_g G S_n + \frac{\rho_n V_n C_{pn}}{\Delta t} T_{n,i}^n \tag{30}$$

$$B_3 = \frac{\rho_f V_f C_{pf}}{\Delta t} T_{f,i}^n + \frac{\rho_f V_f C_{pf} u_f}{\Delta x} T_{f,i-1}^{n+1} \tag{31}$$

$$B_4 = \frac{\rho_p V_p C_{p_p}}{\Delta t} T_{p,i}^n + h_{ci} S_p T_{amb} \tag{32}$$

The matrix equation can therefore be solved in the form: $[T] = [A]^{-1} \times [B]$

The temperature-dependent physical properties of the fluid are calculated using the average temperature of the fluid flowing through the tubes. These equations were solved using an iterative method with the SCILAB simulation software (version 6.1). This allows the temperature of the various components of the solar collector to be calculated at each time step.

Efficiency of solar collector: The efficiency of a collector is one of the criteria used to determine the performance of a solar collector. It is defined, based on the analysis carried out by Hottel, Willier, Wortz and Bliss, as the ratio of the thermal energy received by the heat transfer fluid to the thermal energy received from the sun ((14), (15)).

$$\eta = \frac{Q_u}{S_g G} = \frac{\dot{m}_f C_{pf}\left(T_{fs} - T_{fe}\right)}{S_g G} \tag{33}$$

Where Q_u is the amount of useful heat collected by the collector, expressed in W,G is the total solar radiation falling on the collector's surface in W/m^2. The term $\dot{m}_f$ is the mass flow rate of the heat transfer fluid entering the can tubes. It is expressed in g/s .

RESULTS AND DISCUSSION

Validation of the numerical model of the solar collector: The mathematical model developed was validated using experimental data obtained from the experiment. The model compares the theoretical outlet air temperature with the experimental temperature, as well as the instantaneous thermal efficiency. Figure 4 shows the variation in solar radiation and ambient temperature over time. The experimental data for ambient temperature and solar radiation were obtained on 31 March 2023. These data have been smoothed, and the resulting values are used as input conditions for the collector simulation.

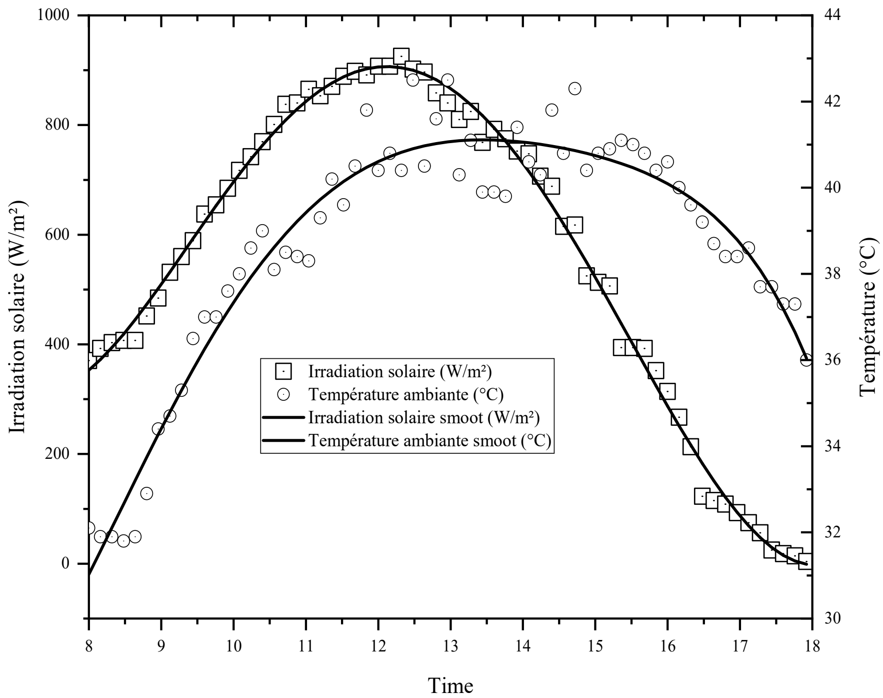

Figure 4. Total sunshine and ambient temperature

In order to validate the model for the solar collector, a comparison was made between the simulated outlet temperature of the solar collector and the experimentally measured temperature. Figure 5 shows the variation in the experimental and theoretical outlet air temperatures of the solar collector. The results show that the theoretical temperature profile at the solar collector outlet is very close to the experimental one.Furthermore, the relative error betweenthe simulation results and the experimental data for the air temperature measurements at the solar collector outlet are given by the statistical parameters such as: $R^2 = 0.92$; RMSE = 0.024 and SSE = 0.018, allow us to conclude that the model adequately describes the thermal behaviour of our solar collector.

Figure 6 shows the trends in the experimental and theoretical values for the instantaneous thermal efficiency of the solar collector. An air flow rate of 0.0109 kg/s was used as the input data. Observation of the figure shows that the two curves exhibit the same rising trends. However, some discrepancies exist, particularly at the beginning and towards the end of these curves. This may be due to fluctuations in sunlight caused by cloud cover observed during the experiment.The maximum instantaneous efficiency value obtained from the simulation is 0.298, which is very close to that derived from the experiment, which is 0.303 for a maximum average irradiance of 925 W/m². The model therefore provides a reasonable prediction of the solar collector's thermal behaviour. The relative errors between the simulation results and the experimental data for this efficiency are given by the statistical parameters: $R^2 = 0.89$; RMSE = 0.022 and SSE = 0.11. The values of these statistical parameters confirm that the model provides a reasonable estimate of the collector's efficiency.

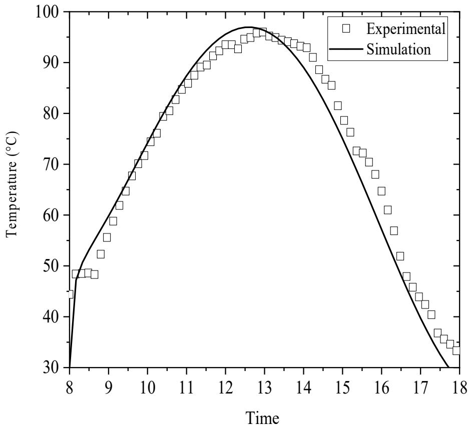

Figure 5 . Comparison of theoretical and experimental temperature profiles of the air at the solar collector outlet

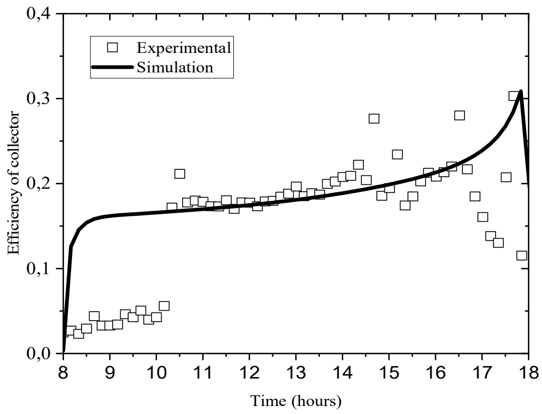

Figure 6. Comparison of the theoretical and experimental thermal efficiency of the solar collector

Measurement of the temperatures of the various components of the solar collector: Figure 7 shows the variation in the theoretical temperatures of the various components of the collector such as the glass, the absorber, the heat transfer fluid and the ambient temperature over time. Looking at these figures, it can be seen that all these temperatures follow the same pattern and reach their maximum between 12 and 1 pm. It can be seen that the absorber temperature is the highest, this can be explained by its high solar absorption coefficient (the absorber is made of black-painted aluminum cans, i.e. it has a selective coating of 0.95).Then occurs the heat transfer fluid high temperature due to convective exchange coefficient between the absorber (aluminum can) and the heat transfer fluid, but also resulting in three (03) holes at each can outlet which rise the turbulence and improve the thermal exchange. Next,comes the temperature of the glass pane, the low temperature of the glass pane compared to the two previous ones can probably be due to its low absorption coefficient (α_g=0.02) and also resulting in the wind on the glass pane surface which entails thermal losses through convection with the ambient air. Finally, the ambient temperatureremains the lowestthroughout the day.

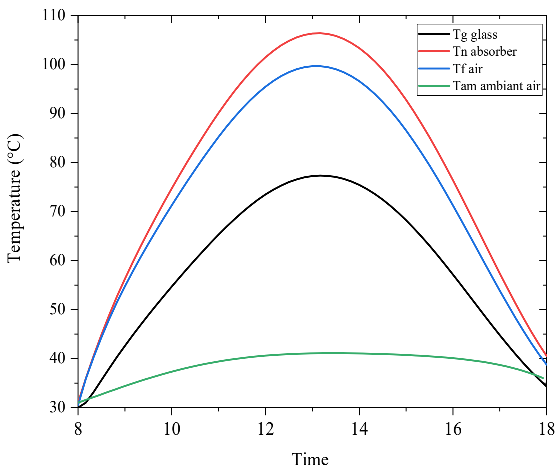

Figure 7. Temperature profiles of the various components of the solar collector

Effect of air mass flow rate on the temperature of the heat transfer fluid and the efficiency of the solar collector: In general, the mass flow rate of the heat transfer fluid is one of the most important parameters influencing the thermal performance of solar collectors. Figure 8 shows the variation in the air temperature at the outlet of the solar collector as a function of ma ss flow rate over time. The results show that the outlet temperature of the heat transfer fluid increases as the flow rate decreases, a finding confirmed by studies conducted by Donatien Njomo et al(15). This can be explained by the fact that as the air flow rate increases, the volume of air to be heated using the same amount of solar energy increases, leading to a decrease in the air temperature at the outlet of the collector. Figure 9 illustrates the effect of variations in the mass air flow rate per unit area on the daily thermal output at time t_M = 12:00 for the three-hole (03) can tubes. It can be seen that the solar collector’s output increases as the air flow rate increases. This demonstrates that convective heat transfer between the air and the inner walls of the can tubes improves significantly as the air flow rate at the inlet to the can tube columns increases; furthermore, the residence time of the heat transfer fluid inside these tubes decreases, which also leads to a reduction in heat losses.

Effect of the length of the can tube columns on the temperature of the heat transfer fluid: Figure 10 shows how the temperature of the heat transfer fluid at the outlet of the solar collector varies with the length of the fluid flow tube. It can be seen that the fluid temperature is proportional to the length of the absorber tube. As the intensity of solar radiation increases, the fluid temperature rises rapidly and decreases gradually as the intensity of solar radiation decreases.

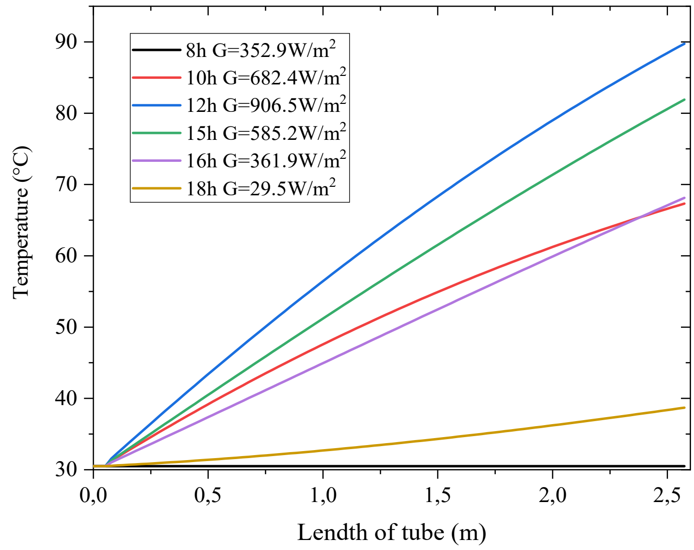

Figure 10. Fluid temperature profiles as a function of the length of the can-tube columns

Effect of the number of holes on the temperature of the heat transfer fluid and the efficiency of the collector: Figure 11 shows the effect of varying the number of holes at the outlet of each can tube on the fluid outlet temperature. The estimated temperature profiles show a decrease in fluid temperature at the solar collector outlet (except for one (01) 1 cm diameter hole) as the number of holes increases. This demonstrates that as the number of holes increases, the heat transfer surface area decreases, leading to reduced turbulence, which in turn results in a decrease in the convective heat transfer coefficient. The can tubes with one (01) 1 cm diameter hole exhibit a lower temperature profile than those with two (02) 1 cm diameter holes. This may be due to heat losses caused by the residence time of the heat transfer fluid, which becomes prolonged inside the columns of can tubes with 1 cm diameter holes. Figure 12 shows the variation in daily thermal efficiency as a function of the number of holes in the can tubes at time t_M. The data show an increase in efficiency from one (01) to two (02) holes, followed by a rapid decrease beyond two (02) holes. The highest efficiency is achieved for can tubes with two (02) holes. This demonstrates that an increase in the number of holes leads to a reduction in the heat transfer coefficient, resulting in a decrease in the solar collector's efficiency. The lower efficiency of cans with one hole compared to those with two holes may be due to heat losses caused by the prolonged residence of the heat transfer fluid inside the can tubes.

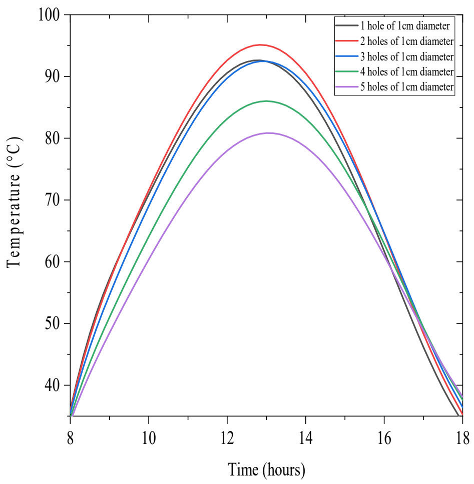

Figure 11. Effect of the number of holes on the outlet fluid temperature profile

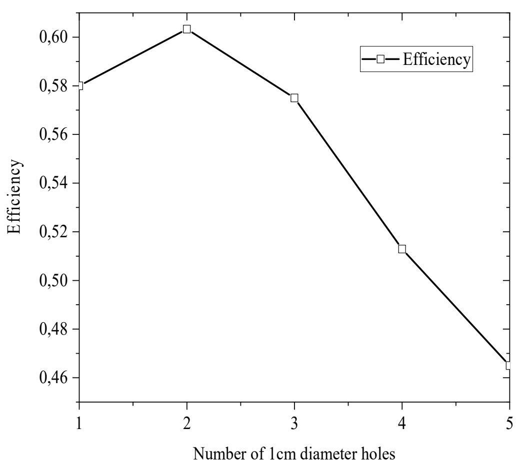

Figure 12. Effect of the number of holes on the daily thermal output of the solar collector at time t_M

Effect of the number of holes on the heat transfer coefficient between the heat transfer fluid and the inner walls of the can columns: Figure 13 illustrates the relationship between the theoretical convective heat transfer coefficient between the heat transfer fluid and the inner walls of the can-tube columns for different numbers of holes over time. The results obtained show that the heat transfer coefficient decreases as the number of holes increases. This indicates that as the number of holes increases, the heat exchange surface area and turbulence within the tube bundles decrease, leading to a reduction in the heat transfer coefficient .

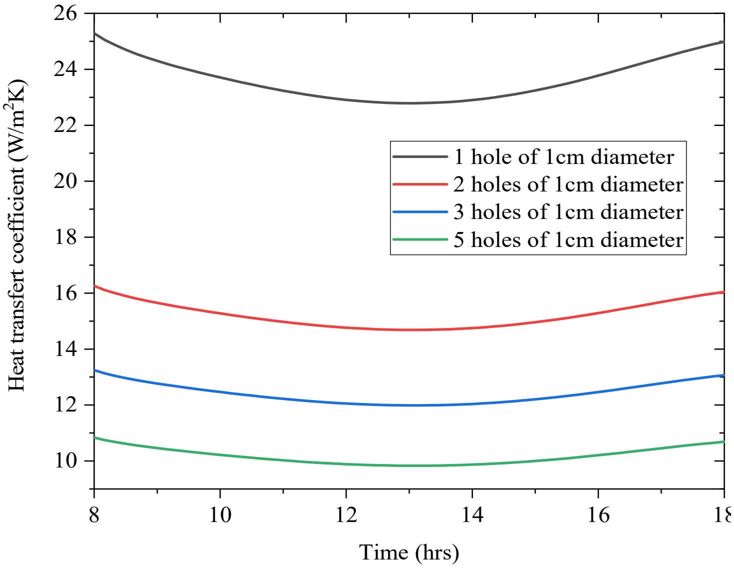

Figure 13 :Effect of the number of holes on the convective transfer coefficient

CONCLUSION

Through this study, we have succeeded in developing a numerical model capable of describing the thermal behaviour of an air solar collector under transient conditions. A comparison of the theoretical and experimental results shows that the simulation model provides a good approximation of reality, despite some climatic disturbances (clouds). Following its validation, the model was used to determine the influence of certain parameters, such as the mass flow rate of the fluid, the length of the columns of can tubes, and the number of 1 cm diameter holes at the outlet of each can. The results show that:

- The outlet temperature of the heat transfer fluid decreases as the air flow rate at the solar collector inlet increases;
- The daily thermal efficiency increases as the air flow rate at the solar collector inlet increases;
- The outlet fluid temperature increases as the length of the finned tube columns and solar irradiance increase;
- The system performs optimally with finned tubes having two (02) 1 cm diameter holes, in terms of both outlet fluid temperature and efficiency

Nomenclature

C_p	heat capacity (J/kg.K)
D_c	tube diameter (m)
e	thickness (m)
G	solar global radiation (W/m^2)
h_r	radiation exchange coefficient (W/m^{2}K)
h_v	convection exchange coefficient (W/m^{2}K)
h_{ci}	conduction exchange coefficient (W/m^{2}K)
$\dot{m}_f$	mass flow rate (kg/s)
Nu	Nusselt number
Pr	Prandlt number
Q_u	useful heat gain of collector, (W)
Ra	Rayleigh number
Re	Reynold number
S	area (m^2)
S_{n-f}	fluid-absorber exchange surface (m^2)
t	time (s)
T	temperature (K)
u_f	fluid velocity (m/s)
u_{amb}	ambient air velocity (m/s)
U_{av}	forward heat loss coefficient (W/m^{2}K)
U_{ar}	rear heat loss coefficient (W/m^{2}K)
U_L	overall heat loss coefficient (W/m^{2}K)
V	volume (m^3)

Greek symbols	
α	absorptance coefficient (-)
μ	dynamic viscosity (kg/m.s)
κ	thermal diffusivity (m^2/s)
ν	kinematic viscosity (m^2/s)
ρ	density (kg/m^3)
λ	thermal conductivity (W/m K)
τ	transmittance coefficient of glass
ε	emissivity (-)
η	thermal efficiency of collector
σ	Stefan–Boltzman constant (W/m^2 K^4)
Subscripts	
amb	ambiant
g	glass
f	fluid (air)
fe	fluid at the inlet
fs	fluid at the outlet
p	plate
n	absorber
ac	stagnant air
iso	isolation
sky	sky

REFERENCES

Aissaoui, F. A. H. Benmachiche, A. Brima, D. Bahloul, and Y. Belloufi, "Experimental and theoretical analysis on thermal performance of the flat plate solar air collector," *Int. J. Heat Technol.*, vol. 34, no. 2, pp. 213–220, 2016, doi: 10.18280/ijht.340209.

Ma, J. W. Sun, J. Ji, Y. Zhang, A. Zhang, and W. Fan, "Experimental and theoretical study of the efficiency of a dual-function solar collector," *Appl. Therm. Eng.*, vol. 31, no. 10, pp. 1751–1756, 2011, doi: 10.1016/j.applthermaleng.2011.02.019.

Pakdaman, M. F. A. Lashkari, H. B. Tabrizi, and R. Hosseini, "Performance evaluation of a natural-convection solar air-heater with a rectangular-finned absorber plate," *Energy Convers. Manag.*, vol. 52, no. 2, pp. 1215–1225, 2011, doi: 10.1016/j.enconman.2010.09.017.

Gao, W. W. Lin, and E. Lu, "Numerical study on natural convection inside the channel between the ¯ at-plate cover and sine-wave absorber of a cross-corrugated solar air heater," vol. 41, pp. 145–151, 2000.

Goldstein L. and E. M. Sparrow, "Experiments on the Transfer Characteristics of a Corrugated Fin and Tube Heat Exchanger Configuration," no. February 1976, pp. 26–34, 1976.

Hegazy, A. A. "Performance of flat plate solar air heaters with optimum channel geometry for constant / variable flow operation," vol. 41, pp. 401–417, 2000.

Abene, A. V. Dubois, M. Le Ray, and A. Ouagued, "Study of a solar air flat plate collector: Use of obstacles and application for the drying of grape," *J. Food Eng.*, vol. 65, no. 1, pp. 15–22, 2004, doi: 10.1016/j.jfoodeng.2003.11.002.

Yeh, H. C. Ho, and J. Hou, "Collector efficiency of double-flow solar air heaters with fins attached," vol. 27, pp. 715–727, 2002.

Ozgen, F. M. Esen, and H. Esen, "Experimental investigation of thermal performance of a double-flow solar air heater having aluminium cans," *Renew. Energy*, vol. 34, no. 11, pp. 2391–2398, 2009, doi: 10.1016/j.renene.2009.03.029.

Sinon, S. S. Tera, and O. Sanogo, "Experimental Investigation for Augmentation of Thermal Performance of Solar Air Collector," vol. 11, no. 3, pp. 1–8, 2023, doi: 10.9734/AJOPACS/2023/v11i3201.

McAdams W. H., Heat Transmission, 3rd edn. McGrawHill, New York (1954).

Hollands K. G. T., Unny T. E., Raithby G. R. and Konicek L. Free convective heat transfer across inclined air layers, Trans. ASME, J. Heat Transfer 98, 189-193 (1976).

Swinbank W. C., Long-wave radiation from clear skies, Q. J. R. Meteorol. Sot. 89, 339 (1963).

Ong KS. Thermal performance of solar air heaters: mathematical model and solution procedure. Solar Energy 1995;55(2):93–109.

Njomo D. and M. Daguenet, "Sensitivity analysis of thermal performances of flat plate solar air heaters," *Heat Mass Transf. und Stoffuebertragung*, vol. 42, no. 12, pp. 1065–1081, 2006, doi: 10.1007/s00231-005-0063-9.

****